

Inactivation of p53 provides a competitive advantage to del(5q) myelodysplastic syndrome hematopoietic stem cells during inflammation

Tomoya Muto,^{1,2} Callum S. Walker,¹ Puneet Agarwal,¹ Eric Vick,³ Avery Sampson,¹ Kwangmin Choi,¹ Madeline Niederkorn,¹ Chiharu Ishikawa,^{1,4} Kathleen Hueneman,¹ Melinda Varney⁵ and Daniel T. Starczynowski^{1,4,6,7}

¹Division of Experimental Hematology and Cancer Biology, Cincinnati Children's Hospital Medical Center, Cincinnati, OH, USA; ²Department of Hematology, Chiba University Hospital, Chiba, Japan; ³Division of Hematology and Oncology, University of Cincinnati, Cincinnati, OH, USA; ⁴Department of Cancer Biology, University of Cincinnati, Cincinnati, OH, USA; ⁵Department of Pharmaceutical Science and Research, Marshall University, Huntington, WV, USA; ⁶Department of Pediatrics, Cincinnati Children's Hospital Medical Center, Cincinnati, OH, USA and ⁷UC Cancer Center, Cincinnati, OH, USA

Correspondence: D. Starczynowski
Daniel.Starczynowski@cchmc.org

T. Muto
Tomoya.Muto@chiba-u.jp

Received: November 2, 2022.

Accepted: April 17, 2023.

Early view: April 27, 2023.

<https://doi.org/10.3324/haematol.2022.282349>

©2023 Ferrata Storti Foundation

Published under a CC BY-NC license



Abstract

Inflammation is associated with the pathogenesis of myelodysplastic syndromes (MDS) and emerging evidence suggests that MDS hematopoietic stem and progenitor cells (HSPC) exhibit an altered response to inflammation. Deletion of chromosome 5 (del(5q)) is the most common chromosomal abnormality in MDS. Although this MDS subtype contains several haploinsufficient genes that impact innate immune signaling, the effects of inflammation on del(5q) MDS HSPC remains undefined. Utilizing a model of del(5q)-like MDS, inhibiting the IRAK1/4-TRAF6 axis improved cytopenias, suggesting that activation of innate immune pathways contributes to certain clinical features underlying the pathogenesis of low-risk MDS. However, low-grade inflammation in the del(5q)-like MDS model did not contribute to more severe disease but instead impaired the del(5q)-like HSPC as indicated by their diminished numbers, premature attrition and increased p53 expression. Del(5q)-like HSPC exposed to inflammation became less quiescent, but without affecting cell viability. Unexpectedly, the reduced cellular quiescence of del(5q) HSPC exposed to inflammation was restored by p53 deletion. These findings uncovered that inflammation confers a competitive advantage of functionally defective del(5q) HSPC upon loss of p53. Since TP53 mutations are enriched in del(5q) AML following an MDS diagnosis, increased p53 activation in del(5q) MDS HSPC due to inflammation may create a selective pressure for genetic inactivation of p53 or expansion of a pre-existing TP53-mutant clone.

Introduction

Myelodysplastic syndromes (MDS) are clonal hematopoietic stem and progenitor cell (HSPC) malignancies defined by blood cytopenia, myeloid cell dysplasia, and ineffective hematopoiesis. Another underlying feature of MDS is the contribution of inflammation.¹⁻³ The MDS bone marrow (BM) niche exhibits increased inflammatory signaling, including elevated cytokines, chemokines, and alarmins. Microenvironmental alterations are partly due to aging, but there is also evidence that MDS hematopoietic cells themselves alter the stem-cell niche through activation of the innate immune system and related inflammatory signaling. Indeed, inflammation can suppress HSPC fitness, such as through reducing self-renewal or promoting differentiation, leading to selection of various oncogenic events during myeloid leukemogenesis.⁴⁻⁷ Re-

cently, several studies have implicated that low-grade inflammation favors the expansion of pre-leukemic or MDS hematopoietic stem cells (HSC) over normal HSC.⁸⁻¹² Thus, inflammation in MDS has pleiotropic effects on the etiology of the disease.

Hemizygous deletion of the long arm of chromosome 5q (del(5q)) is the most common cytogenetic alteration in MDS. Del(5q) is also found in 25% of therapy-related MDS cases and is strongly correlated with progression to AML.¹³⁻¹⁵ Patients with a sole deletion of 5q exhibit macrocytic anemia, leukopenia, and increased platelets. BM from these patients show dysplastic mononuclear megakaryocytes, erythroid hypoplasia, and low blasts (<5%). Haploinsufficiency of several chr 5q genes have been implicated in del(5q) MDS, including genes that play important roles in ribosome function (RPS14), cell cycle regulation (CDC25c/PP2A), innate immune signaling (miR-

145, miR-146a, TIFAB, and DIAPH), stress response signaling (EGR1), and β -catenin signaling (APC, CSNK1A1). Deletion of RPS14 results in a p53-dependent defect in erythropoiesis, but not in a competitive advantage of HSPC.¹⁶ Moreover, loss of RPS14 coincides with increased expression of alarmins and hematopoietic defects associated with non-cell autonomous innate immune signaling.^{17,18} Genetic barcoding revealed that CSNK1A1 haploinsufficiency is a driver of clonal expansion of del(5q) MDS HSPC.¹⁹ Deletion of miR-145, miR-146a, mDia1, and TIFAB collectively contribute to increased innate immune signaling in MDS HSPC, albeit through distinct mechanisms. Deletion of mDia1 increases innate immune signaling in neutrophils due to upregulation of CD14 and results in an MDS-like phenotype in mice.²⁰ Deletion of miR-145, results in derepression of Mal/TIRAP, which is important for an initial step of signaling by the Toll-like receptor (TLR) superfamily.^{21,22} Deletion of miR-146a increases TRAF6 and IRAK1 mRNA and protein translation, while loss of TIFAB increases TRAF6 protein stability, thus resulting in activation of TRAF6 and IRAK1 in MDS HSC even in the absence of ligand-mediated activation of TLR.²²⁻³⁰ Reduced TIFAB expression also results in diminished USP15 de-ubiquitinase function and consequently p53 activation in hematopoietic cells.³¹ Concurrent hematopoietic-specific deletion of TIFAB and miR-146a results in higher levels of TRAF6 expression and innate immune pathway activation, which coincides with a highly penetrant BM failure, a diseased phenotype that more faithfully recapitulates human del(5q) MDS.²⁵

Despite overwhelming evidence of chronic inflammation in del(5q) MDS patients, the effects of low-grade inflammatory signals on del(5q) MDS HSPC and disease progression remains uncharacterized. In this study, we focused on the effects of low-grade inflammation in del(5q) MDS by utilizing a mouse model with co-deletion of miR-146a and TIFAB, two mediators of aberrant innate immune signaling in del(5q) MDS HSPC. We found that low-grade inflammation suppresses del(5q) MDS HSPC via p53 and provide a potential explanation for the high rate of TP53 mutations in patients with del(5q).

Methods

Materials

Lipopolysaccharide (LPS) (L6529) and LPS-EB Ultrapure (TLRL-PEKLPS) were purchased from Sigma and InvivoGen, respectively. The IRAK1/4 inhibitor (NCGC-1481) has been previously described.^{32,33} UBE2N inhibitor (UC-764865) has been previously described.³⁴ MDS-L cells have been previously described.^{35,36}

Mice

miR-146a^{-/-} C57BL/6 mice were obtained from Dr. David Baltimore as previously described.²⁹ Generation of *Tifab*^{-/-};*miR-146a*^{-/-} mice was previously described.^{25,26} *Tifab*^{-/-};*miR-146a*^{-/-} mice were crossed with *Trp53*^{-/-} mice (Jackson Laboratories, 002101). All mouse experiments were performed in accordance with the Association for Assessment and Accreditation of Laboratory Animal Care-accredited animal facility of Cincinnati Children's Hospital. Additional information on the mice can be found in the *Online Supplementary Appendix*.

Bone marrow transplantation

For non-competitive BM transplantations, CD45.2⁺ BM cells were transplanted into lethally-irradiated recipient mice (CD45.1⁺ B6.SJL^{Ptprca} Pep3b/Boy; 6-10 weeks of age). For competitive transplantations, BM cells from 8-week-old CD45.2⁺ BM cells were transplanted with WT CD45.1⁺ BM cells (10:1 ratio) into lethally irradiated CD45.1⁺ recipient mice. For serial transplantation, BM cells were collected from all recipient mice 3 months after transplantations, pooled together, and then BM cells were transplanted into lethally-irradiated recipient mice (CD45.1⁺ B6.SJL^{Ptprca} Pep3b/Boy; 6-10 weeks of age). Detailed information on BM transplantations has been previously reported.³⁷⁻³⁹

Cell cycle and apoptosis analysis

Bromouridine (BrdU) (Sigma-Aldrich) was administered continuously to mice via drinking water (0.5 mg/mL). After 1 week, BrdU incorporation was analyzed using a BrdU Flow Kit (559619, BD Biosciences) according to the manufacturer's recommendation. Annexin V viability staining was carried out according to manufacturer's instructions (C0556419, BD Biosciences).

Additional methods and materials can be found in the *Online Supplementary Appendix*.

Results

Inhibition of IRAK1/4-TRAF6 alleviates cytopenias in *Tifab*^{-/-};*miR-146a*^{-/-} mice

TIFAB and miR-146a are co-deleted in ~80% of del(5q) MDS patients and are both implicated in innate immune and inflammatory signaling. Deletion of miR-146a results in de-repression of TRAF6 and IRAK1 mRNA, while loss of TIFAB increases expression of TRAF6 protein in MDS HSPC (Figure 1A), thus resulting in activation of innate immune pathways.²²⁻³⁰ We utilized a mouse model in which *Tifab* and miR-146a were simultaneously deleted (*Tifab*^{-/-};*miR-146a*^{-/-}), as previously described.²⁵ This model when evaluated in bone marrow (BM) chimeras recapitulates several aspects of del(5q) MDS, including HSPC defects primarily affecting the myeloid lineage, progressive peripheral blood

cytopenias, myeloid dysplasia, and a fatal BM failure in a subset of mice. Moreover, the BM plasma of *Tifab*^{-/-};*miR-146a*^{-/-} mice exhibit an altered cytokine milieu as indicated by elevated expression of IL1a, CXCL1, CXCL2, CXCL5, and CXCL9 and reduced expression of IL15 as compared to BM plasma from wild-type (WT) mice (*Online Supplementary Figure S1A*). As in human del(5q) MDS HSPC, deletion of *Tifab* and *miR-146a* results in activation of IRAK1 and TRAF6 signaling, which directly lead to aberrant HSPC

function.²⁵ Therefore, to determine whether suppressing IRAK1/4-TRAF6 signaling can restore normal blood counts in *Tifab*^{-/-};*miR-146a*^{-/-} mice with cytopenias, we utilized an IRAK1/4 inhibitor (NCGC-1481) and UBE2N inhibitor (UC-764865, or “UC-65”) *in vivo*.^{32,34} The IRAK1/4 inhibitor targets the kinase functions of IRAK1 and IRAK4, while the UBE2N inhibitor targets the ubiquitin-conjugating enzyme (UBE2N) utilized by TRAF6 for signaling. As expected, activation of IRAK1 and NF- κ B signaling in *Tifab*^{-/-};*miR-146a*^{-/-} BM cells

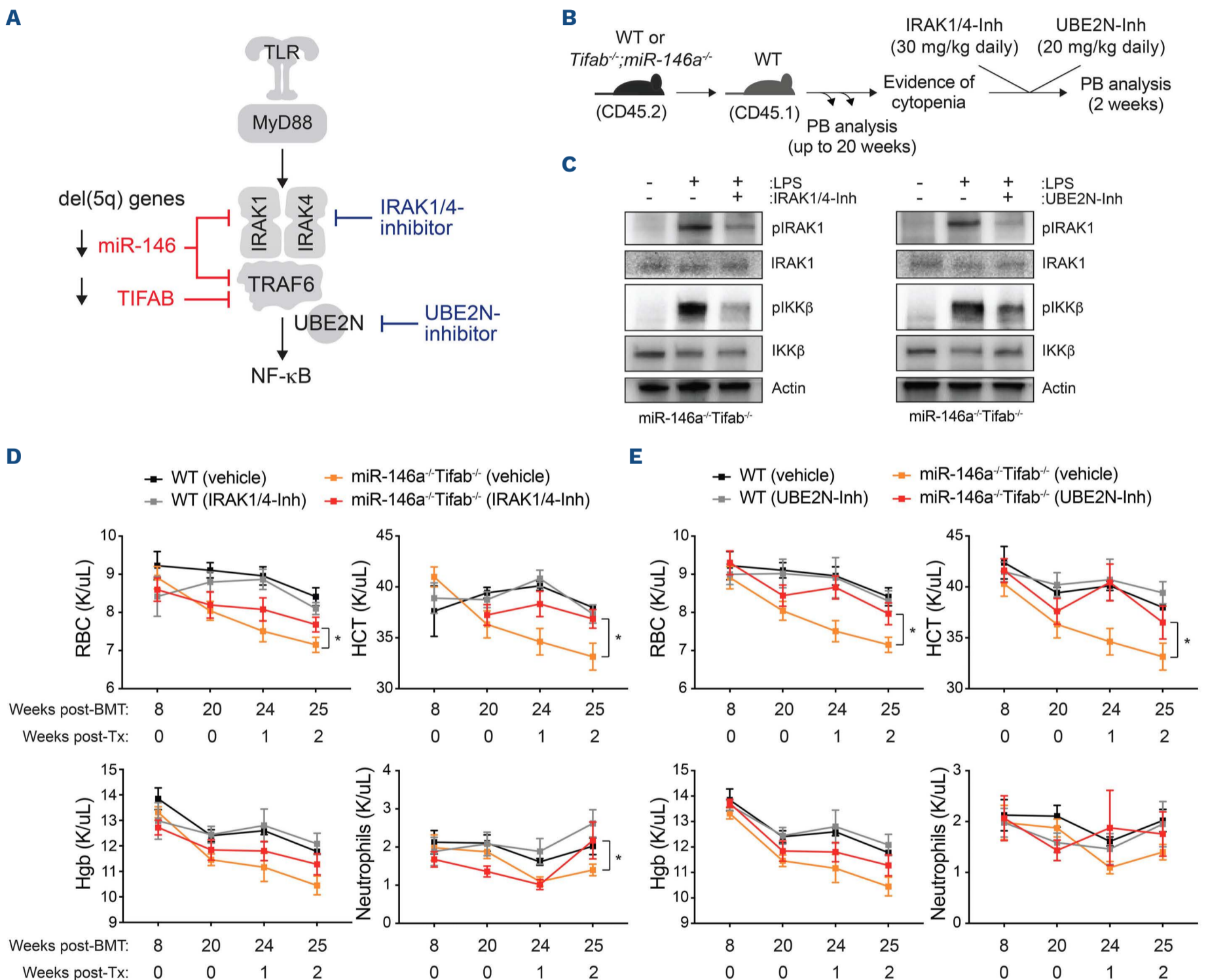


Figure 1. Inhibition of the TRAF6-IRAK1/4 axis restores blood counts in *Tifab*^{-/-};*miR-146a*^{-/-} mice. (A) Overview of del(5q) myelodysplastic syndromes (MDS) resulting in haploinsufficient expression of the 5q- genes *miR-146a* and *TIFAB* and a corresponding increase in expression of their targets, TRAF6 and IRAK1. (B) Immunoblotting of *Tifab*^{-/-};*miR-146a*^{-/-} bone marrow (BM) cells treated with lipopolysaccharide (LPS) (1 mg/mL) and the IRAK1/4 (1 mM) or UBE2N (5 mM) inhibitor for 30 minutes. (C) Outline of BM transplantations using wild-type (WT) or *Tifab*^{-/-};*miR-146a*^{-/-} BM cells. Peripheral blood (PB) analysis was performed monthly on recipient mice to monitor for cytopenias. At onset of cytopenias in the *Tifab*^{-/-};*miR-146a*^{-/-} recipient mice, an IRAK1/4 inhibitor (NCGC-1481 at 30 mg/kg) or UBE2N inhibitor (UC-65 at 20 mg/kg) was administered daily (or phosphate-buffered saline [PBS], vehicle control). PB counts were performed weekly after the treatment was initiated. (D) PB counts of the recipient mice before (20 weeks post BM transplantation) and after treatment (post-Tx) with the IRAK1/4-inhibitor (N=4-5 per group). (E) PB counts of the recipient mice before (20 weeks post BM transplantation) and post-Tx with the UBE2N-inhibitor (N=4-5 per group). Significance for panels (D and E) was determined with a Student's *t* test (**P*<0.05) between treated and vehicle-treated groups.

was suppressed with the IRAK1/4 or UBE2N inhibitors (Figure 1B). BM cells from *Tifab*^{-/-};*miR-146a*^{-/-} or WT mice were transplanted into lethally-irradiated CD45.1 WT mice. Once the *Tifab*^{-/-};*miR-146a*^{-/-} recipient mice developed peripheral blood (PB) cytopenias (~20 weeks post engraftment), the WT and *Tifab*^{-/-};*miR-146a*^{-/-} recipient mice were randomized and treated daily for 2 weeks with the IRAK1/4 inhibitor, UBE2N inhibitor, or vehicle (phosphate-buffered saline [PBS])^{32,33} (Figure 1C). The *Tifab*^{-/-};*miR-146a*^{-/-} recipient mice treated with PBS progressively developed anemia and neutropenia (Figure 1D, E). However, treatment of the *Tifab*^{-/-};*miR-146a*^{-/-} recipient mice with the IRAK1/4 inhibitor or UBE2N inhibitor restored red blood cell counts and hematocrit, and resulted in a modest improvement in neutrophils (Figure 1D, E), suggesting that the cytopenias associated with deletion of TIFAB and miR-146a in del(5q) MDS are partly attributed to increased IRAK1/4-TRAF6 signaling and can be rescued by targeting IRAK1/4 or TRAF6 activation with small molecule inhibitors.

Low-grade inflammation has pleiotropic effects on the disease phenotype of *Tifab*^{-/-};*miR-146a*^{-/-} mice

Since IRAK1/4-TRAF6 signaling mediates inflammatory signals from various immune-related receptors, we next investigated the impact of chronic low-grade inflammation on the pathogenesis of del(5q) MDS. Low-grade inflammation via the TLR/IL1R superfamily is observed in MDS and implicated in the pathogenesis of disease progression. As such, an inflammatory milieu was established using the gram-negative bacterial component LPS, a ligand for TLR4 and activator of IRAK1/4-TRAF6 signaling, which is freely in circulation of leukemia patients, induces systemic inflammation and affects HSPC function.^{40,41} Chronic low-dose (LD) treatment with LPS (1 mg/g, hereafter LD-LPS) was administered via intraperitoneal (i.p.) injection twice a week for 30 days into *Tifab*^{-/-};*miR-146a*^{-/-} or WT mice (Figure 2A). After the last dose of LD-LPS or vehicle, hematopoietic cell chimeric mice were then established by transplanting BM cells from the treated *Tifab*^{-/-};*miR-146a*^{-/-} or WT mice into lethally-irradiated CD45.1 WT mice. As we observed above, mice engrafted with *Tifab*^{-/-};*miR-146a*^{-/-} BM cells developed multilineage cytopenias, including neutropenia, anemia and thrombocytopenia 4 months post-transplant as compared to mice engrafted with WT BM cells (Figure 2B). As expected, the severity of cytopenias following LD-LPS administration in mice engrafted with *Tifab*^{-/-};*miR-146a*^{-/-} BM cells was worse as compared to LD-LPS treated mice engrafted with WT BM cells (Figure 2B). The proportion of myeloid cells (CD11b⁺Gr1⁻) and lymphoid cells (CD3⁺ and B220⁺) in the PB was also significantly reduced following LD-LPS treatment in mice engrafted with *Tifab*^{-/-};*miR-146a*^{-/-} BM cells as compared to WT mice (Figure 2C). However, LD-LPS administration did not contribute to more severe cytopenias in mice engrafted with

Tifab^{-/-};*miR-146a*^{-/-} BM cells as compared to PBS-treated mice (Figure 2B).

In order to evaluate the effects of chronic low-grade inflammation on disease development, we monitored the mice for over 1 year and found that all mice engrafted with *Tifab*^{-/-};*miR-146a*^{-/-} BM cells that were either treated with LD-LPS or vehicle (PBS) succumbed to disease by ~500 days (median survival ~400 days), while the majority of WT mice treated with LD-LPS or PBS were alive at the conclusion of the experiment (median survival not reached)(Figure 2D). Surprisingly, the disease latency or severity were not impacted by LD-LPS in mice with *Tifab*^{-/-};*miR-146a*^{-/-} BM cells. The mice transplanted with *Tifab*^{-/-};*miR-146a*^{-/-} BM cells that were treated with PBS or LD-LPS developed multi-lineage cytopenias, reduced BM cellularity, and splenomegaly, which are consistent with findings of BM failure (Figure 2E; *Online Supplementary Figure S1B-E*). Administration of LD-LPS resulted in slightly lower blood counts in mice transplanted with *Tifab*^{-/-};*miR-146a*^{-/-} BM cells as compared to vehicle-treated mice, but these differences were not significant (Figure 2E). Examination of the hematopoietic stem and progenitor cells showed that *Tifab*^{-/-};*miR-146a*^{-/-} BM cells produce fewer HSC (Lin⁻cKit⁺Sca1⁺CD150⁺CD48⁻) and hematopoietic progenitor cells (HPC) (Lin⁻cKit⁺Sca1⁺ and Lin⁻cKit⁺) than WT BM cells. Treatment with LD-LPS resulted in a slight, albeit not significant, reduction in *Tifab*^{-/-};*miR-146a*^{-/-} HSC and HPC (Figure 2F). In contrast, LD-LPS induced an expansion of WT HPC as expected based on previous studies. Altogether, these observations suggest that chronic low-grade inflammation does not meaningfully contribute to a more severe disease in the del(5q)-like MDS model.

Low-grade inflammation results in impaired *Tifab*^{-/-};*miR-146a*^{-/-} hematopoietic stem and progenitor cells

In order to explore the effects of LD-LPS on *Tifab*^{-/-};*miR-146a*^{-/-} HSPC, we isolated LSK from WT and of *Tifab*^{-/-};*miR-146a*^{-/-} mice treated *in vivo* with chronic LD-LPS, and performed hematopoietic progenitor cell assays in methylcellulose. LD-LPS had minimal effects on WT LSK as compared to vehicle-treated cells but resulted in a significant reduction of colony formation by *Tifab*^{-/-};*miR-146a*^{-/-} LSK (Figure 3A). One of the consequences of low-grade inflammation on HSC is reduced quiescence due to increased cell proliferation.^{42,43} Therefore, we next evaluated the effect of LD-LPS on the total number and cell cycle status of mice injected with LD-LPS (Figure 3B). LD-LPS resulted in significantly reduced number of *Tifab*^{-/-};*miR-146a*^{-/-} HSC (Lin⁻Sca1⁺cKit⁺CD150⁺CD48⁻) in the BM as compared to PBS-treated *Tifab*^{-/-};*miR-146a*^{-/-} mice or WT mice treated with LD-LPS (Figure 3C). The reduction in *Tifab*^{-/-};*miR-146a*^{-/-} HSC in the BM treated with LD-LPS correlated with an increased frequency of BrdU⁺ *Tifab*^{-/-};*miR-146a*^{-/-} HSC

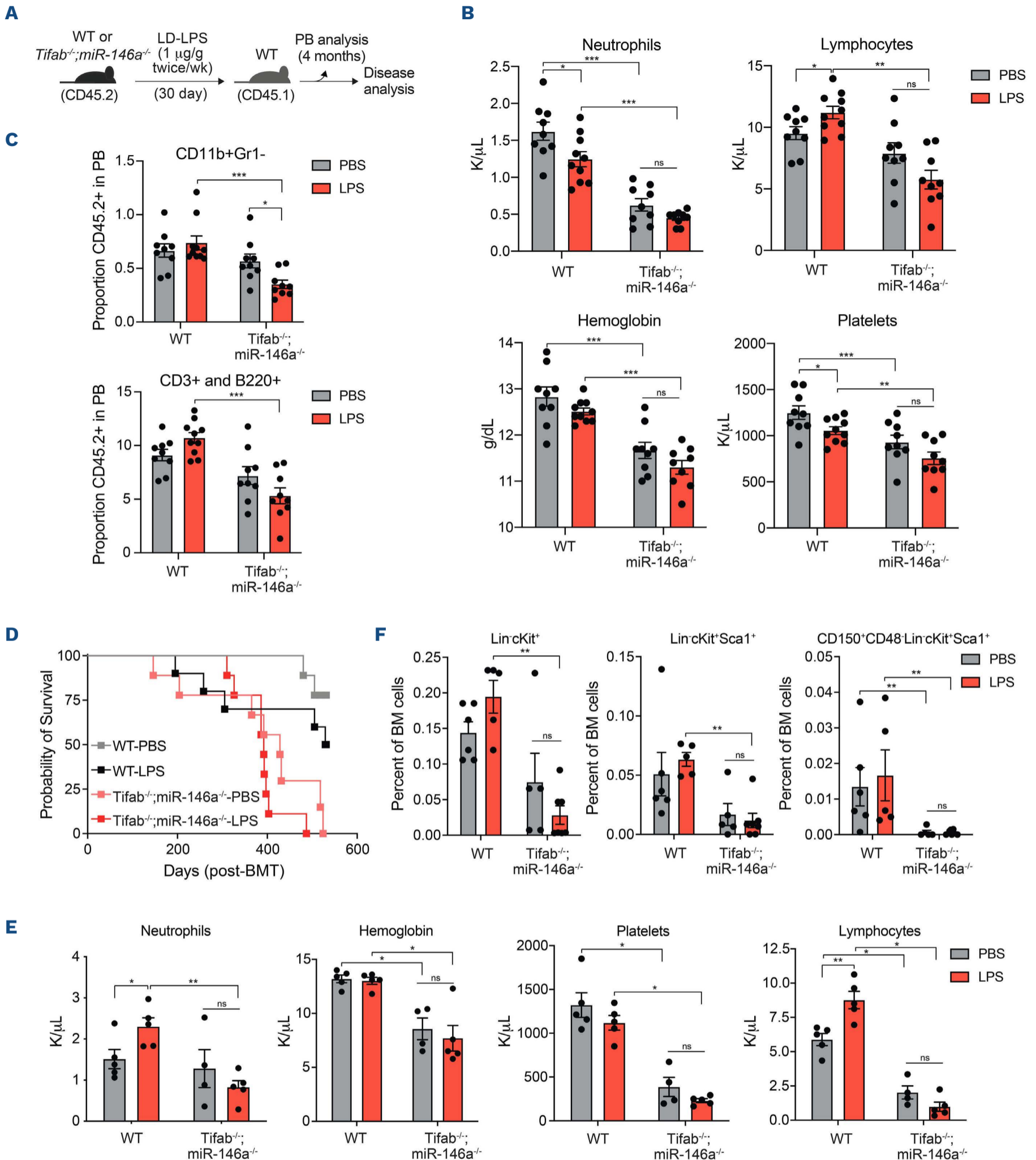


Figure 2. Low-dose lipopolysaccharide does not significantly impact the phenotype of *Tifab*^{-/-};*miR-146a*^{-/-} mice. (A) Outline of bone marrow (BM) transplantations using wild-type (WT) or *Tifab*^{-/-};*miR-146a*^{-/-} mice in the presence of low-dose lipopolysaccharide (LD-LPS). (B) Peripheral blood (PB) counts of the recipient mice at 4 months after transplantation (N=9-10 per group). (C) Summary of lymphoid (CD3⁺ and B220⁺), myeloid (CD11b⁺Gr1⁻) proportions within the PB of the recipient mice (N=9-10 per group). (D) Overall survival of mice transplanted with WT or *Tifab*^{-/-};*miR-146a*^{-/-} mice treated with either PBS or LPS (N=9-10). (E) PB counts of the moribund *Tifab*^{-/-};*miR-146a*^{-/-} mice (N=4-5 per group) at 10-13 months after transplantation. (F) Proportion of the indicated hematopoietic stem and progenitor cells in the BM from moribund *Tifab*^{-/-};*miR-146a*^{-/-} mice (N=5-7 per group). Significance for panels (B, C, E, and F) was determined with a Student's *t* test (**P*<0.05; ***P*<0.01; ****P*<0.001).

cells treated with LD-LPS compared to WT BM cells treated with or without LPS and PBS-treated *Tifab*^{-/-};*miR-146a*^{-/-} BM cells (Figure 3C, D). The reduction in *Tifab*^{-/-};*miR-146a*^{-/-} HSC in the BM after LD-LPS was not due to decreased cell viability. The percent of apoptotic HSC (7AAD/AnnexinV) from *Tifab*^{-/-};*miR-146a*^{-/-} mice treated with LD-LPS was similar to PBS-treated mice or to WT treated with LD-LPS (Figure 3E).

Low-grade inflammation suppresses the long-term competitive advantage of *Tifab*^{-/-};*miR-146a*^{-/-} hematopoietic stem cells

We next investigated the consequences of chronic low-grade inflammation on hematopoiesis and the long-term function of *Tifab*^{-/-};*miR-146a*^{-/-} HSPC *in vivo*. Total BM cells isolated from CD45.2 *Tifab*^{-/-};*miR-146a*^{-/-} or CD45.2 WT mice injected i.p. with LD-LPS twice a week for 30 days and serially transplanted every 4 months with CD45.1 WT competitor BM cells into lethally-irradiated CD45.1 WT

mice (Figure 4A). Exposure to LD-LPS resulted in reduced proportion of CD45.2⁺ *Tifab*^{-/-};*miR-146a*^{-/-} in the PB compared to PBS-derived CD45.2⁺ *Tifab*^{-/-};*miR-146a*^{-/-} PB cells (Figure 4B). The reduction in PB chimerism is mainly due to impaired lymphopoiesis of *Tifab*^{-/-};*miR-146a*^{-/-} cells exposed to LD-LPS (Figure 4C). At this time point, the production of myeloid cells in the PB was increased for *Tifab*^{-/-};*miR-146a*^{-/-} cells exposed to LD-LPS as compared to the control PBS groups following the primary BM transplantation (Figure 4C). Exposure of CD45.2⁺ WT HSPC to LD-LPS resulted in negligible effects at month 3 upon primary BM transplantation (Figure 4C). However, exposure to LD-LPS resulted in reduced proportion of CD45.2⁺ WT cells in PB and CD45.2⁺ WT CD150⁺CD48⁻LSK (LT-HSC) in the BM compared to PBS-derived CD45.2⁺ WT cells at month 3 of the secondary BM transplantation (Figure 4E-G). In stark contrast, CD45.2⁺ *Tifab*^{-/-};*miR-146a*^{-/-} BM cells exposed to LD-LPS resulted in significantly reduced proportions of BM cells compared to PBS-derived CD45.2⁺ BM

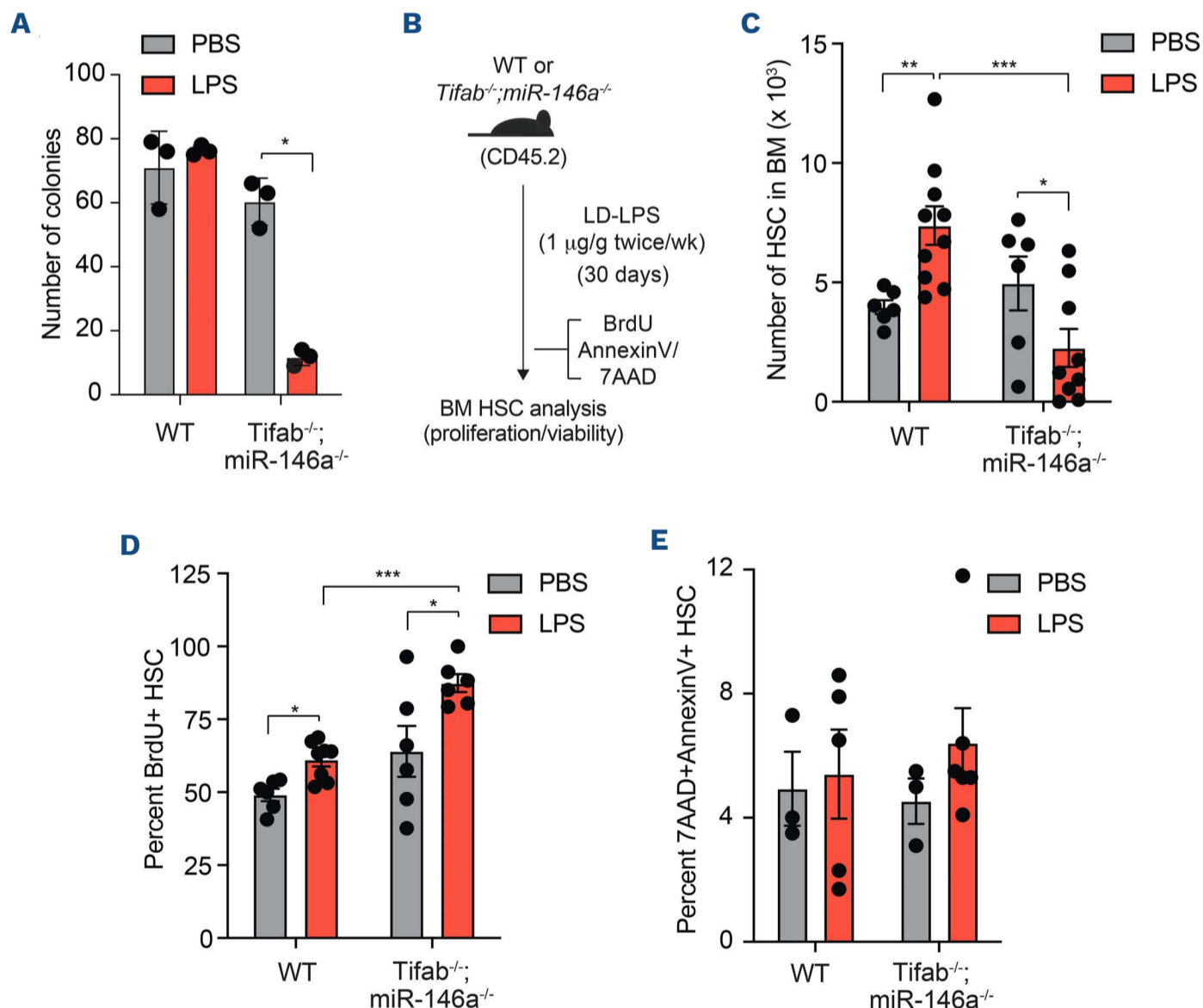
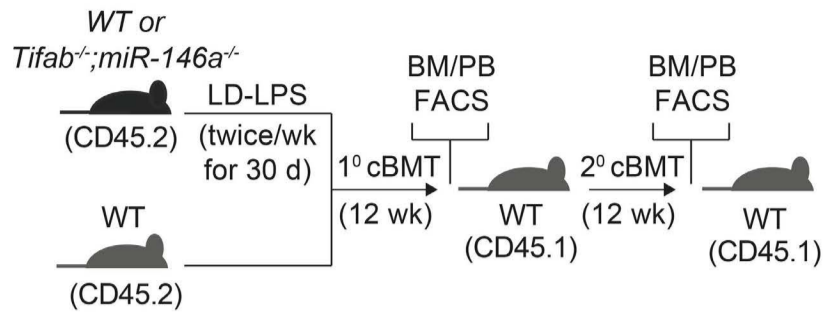


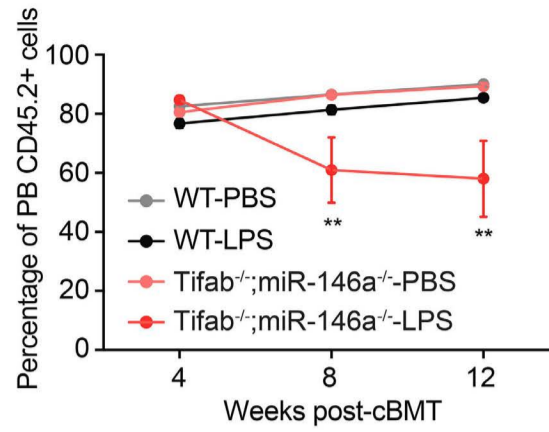
Figure 3. *Tifab*^{-/-};*miR-146a*^{-/-} hematopoietic stem and progenitor cells are less quiescent following low-dose lipopolysaccharide.

(A) Colony assay of wild-type (WT) or *Tifab*^{-/-};*miR-146a*^{-/-} LSK treated with low-dose lipopolysaccharide (LD-LPS) (N=3 per group). (B) Outline of *in vivo* bromouridine (BrdU) incorporation assay using WT and *Tifab*^{-/-};*miR-146a*^{-/-} mice in the presence of low-dose chronic inflammation. (C) Absolute number of hematopoietic stem cells (HSC) from WT and *Tifab*^{-/-};*miR-146a*^{-/-} mice treated with LPS (N=6-10). Error bars represent the standard error of the mean (SEM). (D) Proportion of BrdU-positive cells within HSC from WT and *Tifab*^{-/-};*miR-146a*^{-/-} mice treated with LPS (N=6-8). Error bars represent the SEM. (E) Proportion of 7AAD⁺ AnnexinV⁺ cells within HSC from WT and *Tifab*^{-/-};*miR-146a*^{-/-} mice treated with LPS (N=3-5). Error bars represent the SEM. Significance for panels (C, D, and E) was determined with a Student's *t* test (**P*<0.05; ***P*<0.01; ****P*<0.001).

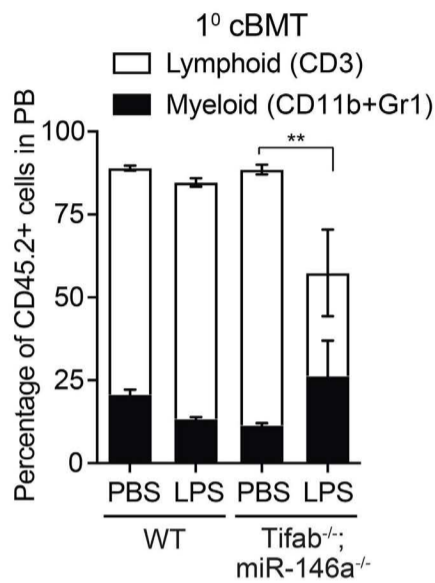
A



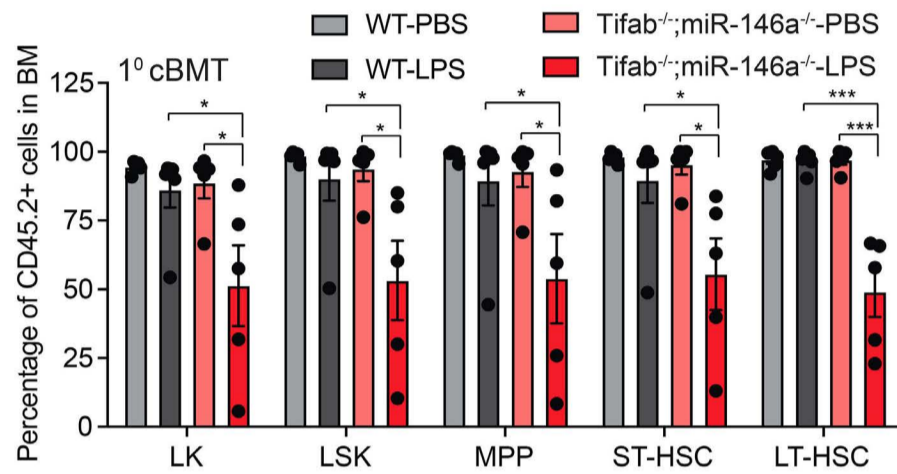
B



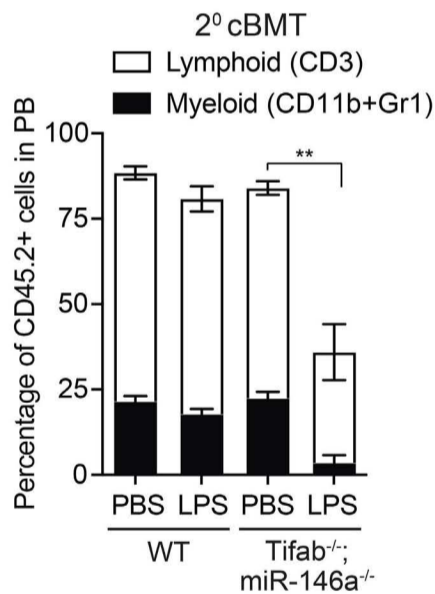
C



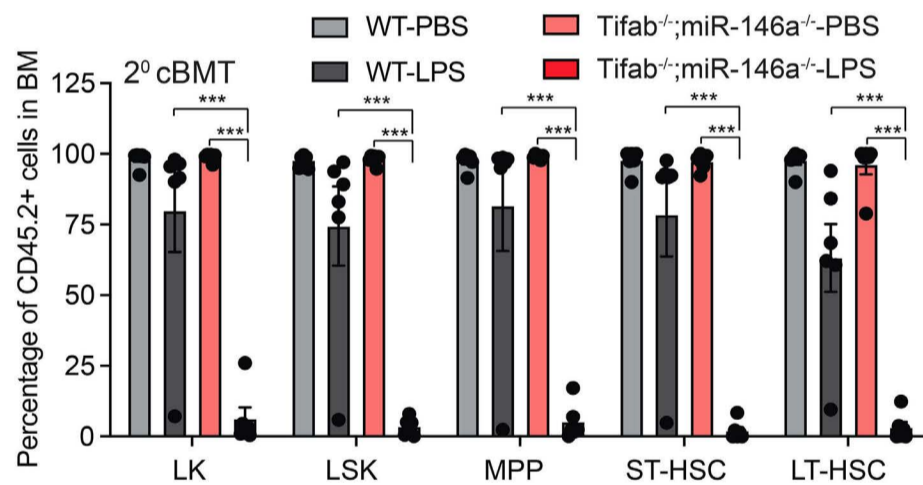
E



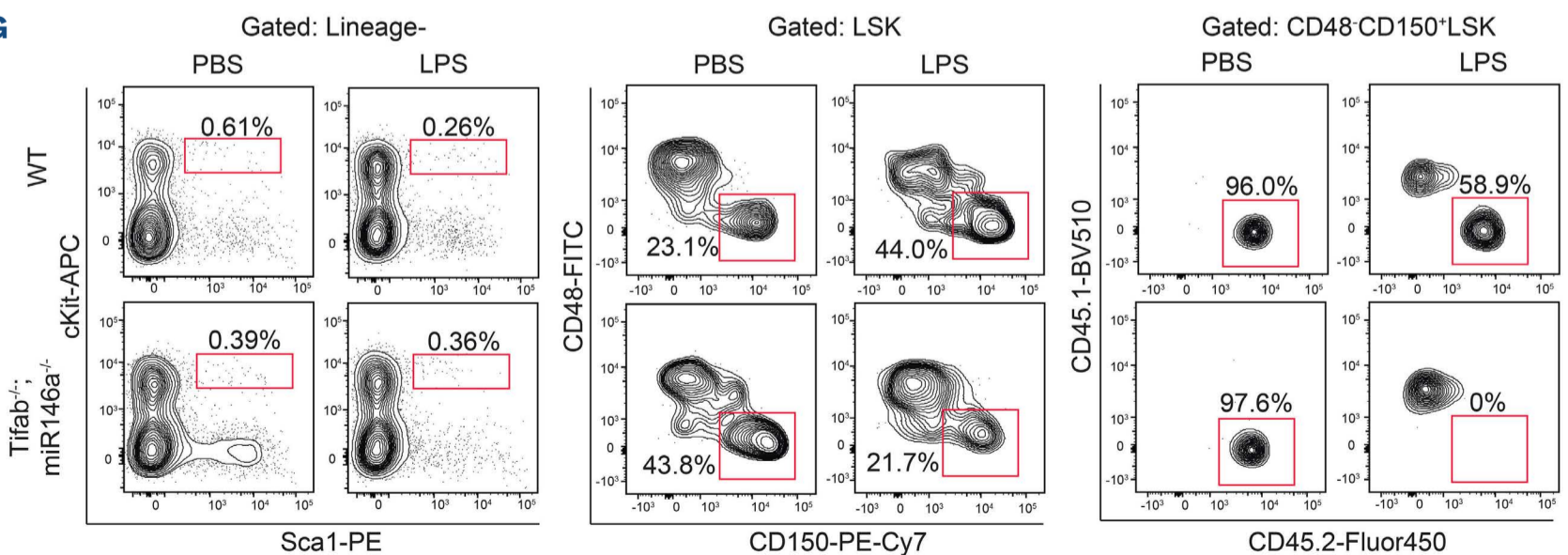
D



F



G



Continued on following page.

Figure 4. *Tifab*^{-/-};*miR-146a*^{-/-} hematopoietic stem and progenitor cells are functionally defective following low-dose lipopolysaccharide. (A) Outline of competitive bone marrow (BM) transplantations using wild-type (WT) or *Tifab*^{-/-};*miR-146a*^{-/-} mice in the presence of low-dose lipopolysaccharide (LD-LPS). (B) Summary of donor-derived peripheral blood (PB) proportions at the indicated time points (N=5-6 per group). Error bars represent the standard error of the mean (SEM). Statistical analysis was performed between *Tifab*^{-/-};*miR-146a*^{-/-}-phosphate-buffered saline (PBS) and -LPS. (C) Proportion of donor-derived PB cells from primary recipient mice (N=5-6 per group). Error bars represent the SEM. (D) Proportions of donor-derived BM cells from primary recipient mice is reported 3 months after transplantation. Error bars represent the SEM (N=5-6 per group). (E) Proportion of donor-derived PB cells from secondary recipient mice (N=6 per group). Error bars represent the SEM. (F) Proportions of donor-derived BM cells from secondary recipient mice is reported 3 months after transplantation. (G) Representative flow cytometric profiles of *Tifab*^{-/-};*miR-146a*^{-/-} and WT BM hematopoietic stem cells (HSC) after the tertiary transplantation. Error bars represent the SEM (N=6 per group). LK: Lin⁻cKit⁺; LSK: Lin⁻cKit⁺Sca1⁺; MPP: multipotent progenitor (Lin⁻cKit⁺Sca1⁺CD48⁺CD150⁻); ST-HSC, Lin⁻cKit⁺Sca1⁺CD48⁻CD150⁻; LT-HSC, Lin⁻cKit⁺Sca1⁺CD48⁻CD150⁺. Significance for panels (B, D, and E) was determined with a Student's *t* test (**P*<0.05; ***P*<0.01; ****P*<0.001).

cells following the primary BM transplantation (Figure 4E). Furthermore, the *Tifab*^{-/-};*miR-146a*^{-/-} BM cells exposed to LD-LPS were unable to recover in the secondary BM transplantation as the proportion of all HSPC subsets were further out-competed by WT cells (Figure 4D-G). Collectively, these results suggest that deletion of *Tifab* and *miR-146a* reduces the long-term repopulating potential of HSPC immediately following inflammation due to loss of cellular quiescence.

Low-grade inflammation results in p53 expression and activation in *Tifab*^{-/-};*miR-146a*^{-/-} hematopoietic stem and progenitor cells

In order to identify the molecular basis for the impaired function of *Tifab*^{-/-};*miR-146a*^{-/-} HSPC during low-grade inflammation, we performed RNA-sequencing in *Tifab*^{-/-};*miR-146a*^{-/-} and WT LSK treated with LD-LPS *in vitro* for 90 min (Figure 5A). LPS treatment resulted in expression of 90 differentially upregulated genes and 212 downregulated genes in *Tifab*^{-/-};*miR-146a*^{-/-} LSK cells compared to vehicle-treated cells (Figure 5B,C; *Online Supplementary Table S1*). In contrast, LPS treatment resulted in 79 upregulated and 125 downregulated genes in WT LSK cells compared to vehicle-treated cells (Figure 5B, C; *Online Supplementary Table S2*). Moreover, there was minimal overlap in the identity of differentially expressed genes in LPS-treated *Tifab*^{-/-};*miR-146a*^{-/-} LSK and WT LSK cells (Figure 5C). Pathway analysis of differentially expressed genes revealed changes in megakaryocyte/platelet- and nicotinic acetylcholine receptor-related pathways in *Tifab*^{-/-};*miR-146a*^{-/-} LSK cells (*Online Supplementary Figure S2*). WT cells treated with LPS exhibited enrichment in pathways related to epigenetic regulation, including histone methylation and acetylation (*Online Supplementary Figure S2*). In order to identify regulatory factors that drive the *Tifab*^{-/-};*miR-146a*^{-/-} HSPC phenotype during low-dose inflammation, we assessed genes that are overexpressed or downregulated in *Tifab*^{-/-};*miR-146a*^{-/-} versus WT LSK following LPS stimulation (Figure 5D). We identified significant enrichment of binding motifs for TP53 (*P*=0.01), GATA2 (*P*=0.006), and RUNX1 (*P*=0.01) in the overexpressed genes from LPS-stimulated *Tifab*^{-/-};*miR-146a*^{-/-} as compared to WT LSK

(Figure 5E). Downregulated genes were not significantly enriched for any specific motif (Figure 5E). These results indicate TLR stimulation of *Tifab*^{-/-};*miR-146a*^{-/-} and WT HSPC results in a distinct effect on gene expression programs, pathways, and cellular states.

We next focused on the potential effects of TP53 signaling in LPS-stimulated *Tifab*^{-/-};*miR-146a*^{-/-} HSPC. In addition to regulating TRAF6, TIFAB also directly binds USP15. One of the key substrates regulated by the TIFAB-USP15 axis includes p53.³¹ Deletion of TIFAB sensitizes hematopoietic cells to a variety of cellular stressors, which are dependent on p53 activation.³¹ Gene set enrichment analysis (GSEA) revealed that a p53-related gene signature was positively enriched in *Tifab*^{-/-};*miR-146a*^{-/-} LSK cells treated with LPS compared to vehicle-treated *Tifab*^{-/-};*miR-146a*^{-/-} cells, while there was no significant enrichment of a p53-related signature in WT cells treated with LPS (Figure 5F). Baseline expression of p53-related genes were comparable between vehicle-treated WT and *Tifab*^{-/-};*miR-146a*^{-/-} HSPC, suggesting that p53 activation occurs during inflammation in del(5q)-like MDS HSPC.

In order to evaluate p53 protein levels in *Tifab*^{-/-};*miR-146a*^{-/-} HSPC exposed to chronic inflammation, we purified cKit⁺ BM cells from WT or *Tifab*^{-/-};*miR-146a*^{-/-} mice that were treated with LD-LPS for 30 days or PBS (Figure 6A). Baseline p53 protein levels were slightly increased in *Tifab*^{-/-};*miR-146a*^{-/-} HSPC as compared to vehicle-treated *Tifab*^{-/-};*miR-146a*^{-/-} HSPC or WT HSPC (Figure 6B). Importantly, p53 protein was further increased upon treatment with LD-LPS in *Tifab*^{-/-};*miR-146a*^{-/-} HSPC as compared to vehicle-treated *Tifab*^{-/-};*miR-146a*^{-/-} HSPC or LPS-treated WT HSPC (Figure 6B). The effects of LPS on p53 expression in *Tifab*^{-/-};*miR-146a*^{-/-} HSPC is dependent on IRAK1/4-TRAF6 activation. *In vitro*-treated *Tifab*^{-/-};*miR-146a*^{-/-} HSPC with LPS resulted in increased p53 protein expression, which was suppressed with the IRAK1/4 or UBE2N inhibitors (Figure 6C). Lastly, to determine whether loss of TIFAB and *miR-146a* in human MDS HSPC exhibit activation of p53, we treated a human del(5q) MDS cell line (MDSL) with LPS. LPS stimulation of MDSL cells resulted in an increase in p53 protein levels (Figure 6D). Moreover, the IRAK1/4 inhibitor suppressed p53 expression upon LPS stimulation (Figure 6E), indicat-

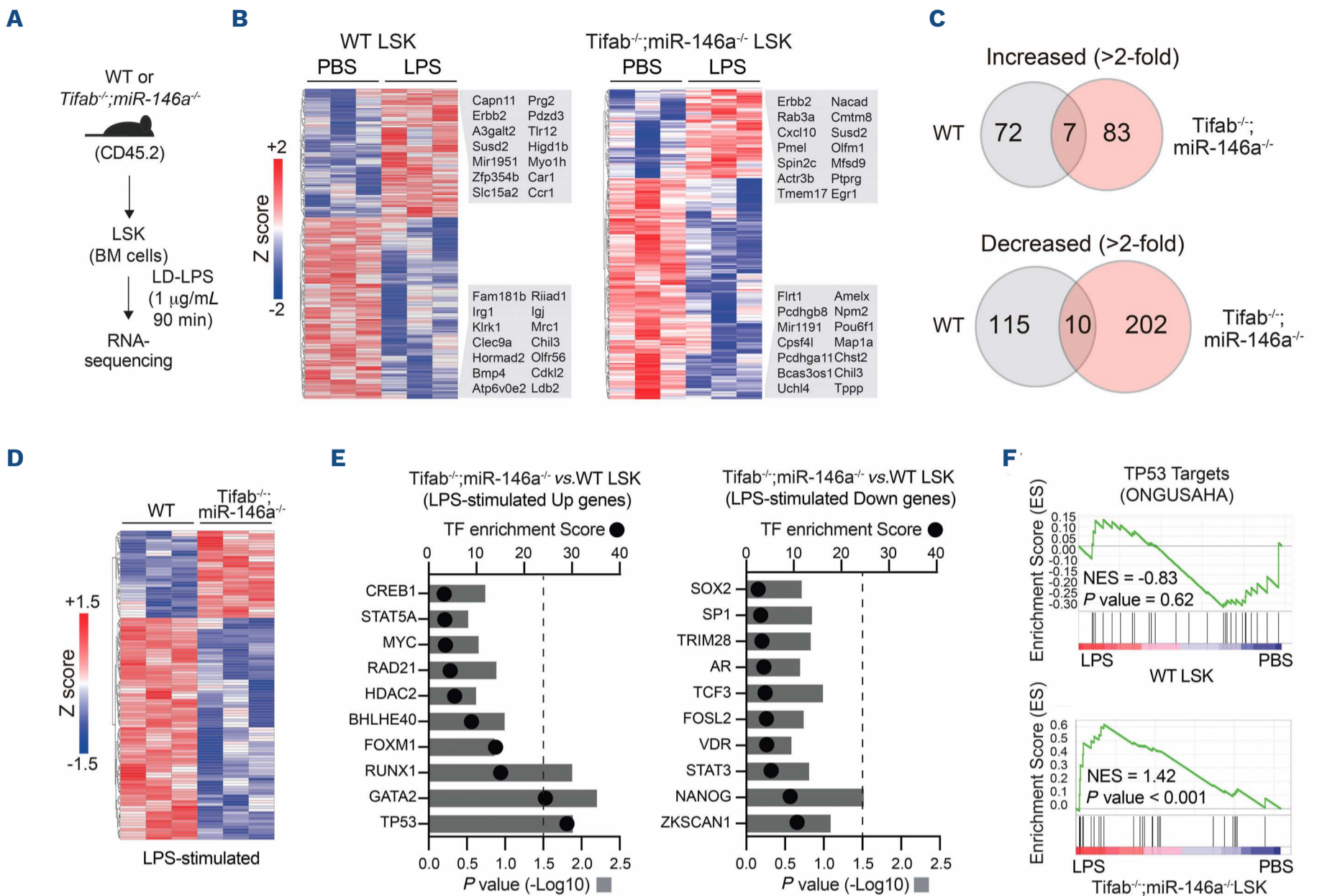


Figure 5. Differential TLR4 stimulation and p53 activation in *Tifab*^{-/-};*miR-146a*^{-/-} hematopoietic stem and progenitor cells with low-dose lipopolysaccharide. (A) Outline of RNA-sequencing using hematopoietic stem and progenitor cells (HSPC) from wild-type (WT) and *Tifab*^{-/-};*miR-146a*^{-/-} mice in the presence of low-dose lipopolysaccharide (LD-LPS). (B) Heatmap of differentially expressed genes in WT or *Tifab*^{-/-};*miR-146a*^{-/-} LSK cells treated with LPS or phosphate-buffered saline (PBS) (1.5-fold; $P < 0.05$; $N = 3$ per group). (C) Venn diagram of upregulated/downregulated genes (1.5-fold; $P < 0.05$) in WT (relative to WT LSK cells treated with PBS) or *Tifab*^{-/-};*miR-146a*^{-/-} LSK cells (relative to *Tifab*^{-/-};*miR-146a*^{-/-} LSK cells treated with PBS). (D) Heatmap of differentially expressed genes in LPS-stimulated WT or *Tifab*^{-/-};*miR-146a*^{-/-} LSK cells (1.5-fold; $P < 0.05$; $N = 3$ per group). (E) Enrichment of transcription factors was determined with the ENCODE and CHIP Enrichment Analysis (ChEA) libraries using genes that are overexpressed (left panel) or downregulated (right panel) in LPS-stimulated *Tifab*^{-/-};*miR-146a*^{-/-} vs. WT LSK. (F) Gene set enrichment analysis plots for TP53 targets in LPS-stimulated WT LSK cells (relative to WT LSK cells treated with PBS) and LPS-stimulated *Tifab*^{-/-};*miR-146a*^{-/-} LSK cells (relative to *Tifab*^{-/-};*miR-146a*^{-/-} LSK cells treated with PBS). NES: normalized enrichment score.

ing that chronic inflammation can directly induce p53 expression via the IRAK1/4-TRAF6 axis. Collectively, these findings suggest that del(5q) MDS HSPC are primed to activate p53 signaling via IRAK1/4-TRAF6 signaling.

Deletion of p53 restores the functional defect of *Tifab*^{-/-};*miR-146a*^{-/-} hematopoietic stem and progenitor cells during low-grade inflammation

TP53 mutations are highly enriched in del(5q) AML patients following an initial MDS diagnosis,⁴⁴ therefore, increased p53 signaling in del(5q) MDS HSPC due to low-grade inflammation may create a selective pressure that eventually leads to genetic inactivation of p53 in the MDS HSPC. In order to examine the role of p53 in *Tifab*^{-/-};*miR-146a*^{-/-}

HSPC during low-grade inflammation, we generated *Tifab*^{-/-};*miR-146a*^{-/-} mice in which one copy of p53 is deleted (*Tifab*^{-/-};*miR-146a*^{-/-};*p53*^{+/-}), which mimics MDS patients with a monoallelic mutation in TP53⁴⁵ (Online Supplementary Figure S3). WT, *Tifab*^{-/-};*miR-146a*^{-/-} or *Tifab*^{-/-};*miR-146a*^{-/-};*p53*^{+/-} mice were treated with LD-LPS or PBS twice a week for 30 days (Figure 7A). After 30 day exposure to LD-LPS, we confirmed that p53 expression was suppressed in *Tifab*^{-/-};*miR-146a*^{-/-};*p53*^{+/-} HSPC as compared to *Tifab*^{-/-};*miR-146a*^{-/-} HSPC (Figure 7B). Following the last treatment with LD-LPS, BM cells (CD45.2) were isolated and co-transplanted with WT competitor BM cells (CD45.1) (one to one ratio) into lethally-irradiated CD45.1 WT mice (Figure 7A). At 5 months post-transplant,

LD-LPS treatment resulted in reduced proportion of *Tifab*^{-/-};*miR-146a*^{-/-} cells in the PB due to impaired production of myeloid cells (Figure 7C, D), as observed in Figure 2C and Figure 4D. In contrast, deletion of p53 restored the PB chimerism of *Tifab*^{-/-};*miR-146a*^{-/-};*p53*^{+/-} myeloid cells exposed to LD-LPS (Figure 7C, D). Furthermore, *Tifab*^{-/-};*miR-146a*^{-/-};*p53*^{+/-} HSC did not decrease in the BM upon LD-LPS treatment as compared to PBS-treated *Tifab*^{-/-};*miR-146a*^{-/-};*p53*^{+/-} HSC, or LD-LPS treated *Tifab*^{-/-};*miR-146a*^{-/-} HSC (Figure 7E). We observed that there were fewer BrdU+ *Tifab*^{-/-};*miR-146a*^{-/-};*p53*^{+/-} HSC upon LD-LPS treatment as compared to *Tifab*^{-/-};*miR-146a*^{-/-} HSC (Figure 7F), suggesting that p53 is responsible for the excessive proliferation of *Tifab*^{-/-};*miR-146a*^{-/-} HSC exposed to low-grade inflammation. Similar findings were observed upon chronic elevation of p53 protein in HSPC.⁴⁶ Although deletion of p53 provides a competitive advantage of *Tifab*^{-/-};*miR-146a*^{-/-} HSPC during low-grade inflammation, we did not observe evidence of aberrant BM morphology nor overt AML in these mice after 1 year (*Online Supplementary Figure S4*

and *data not shown*). Therefore, we posit that p53 mutations preserve the competitive advantage of del(5q) HSPC during chronic low-grade inflammation and that additional cooperating mutations contribute to the development of AML in del(5q) MDS.

Discussion

Inflammation has been shown to favor the expansion of pre-leukemic or MDS HSC over normal HSC and contribute to the pathogenesis of MDS. Based on cytokine profiling of patients with pre-leukemic conditions and MDS, inflammatory cytokine signatures are involved in the early stages of pathogenesis, well before the onset of MDS.⁴⁷ More recently, microbial components, including circulating LPS, have been reported in patients with MDS.⁴⁸ Our study investigated the effects of low-grade chronic inflammation on the function of del(5q)-like mouse MDS HSPC and contribution to disease. Although

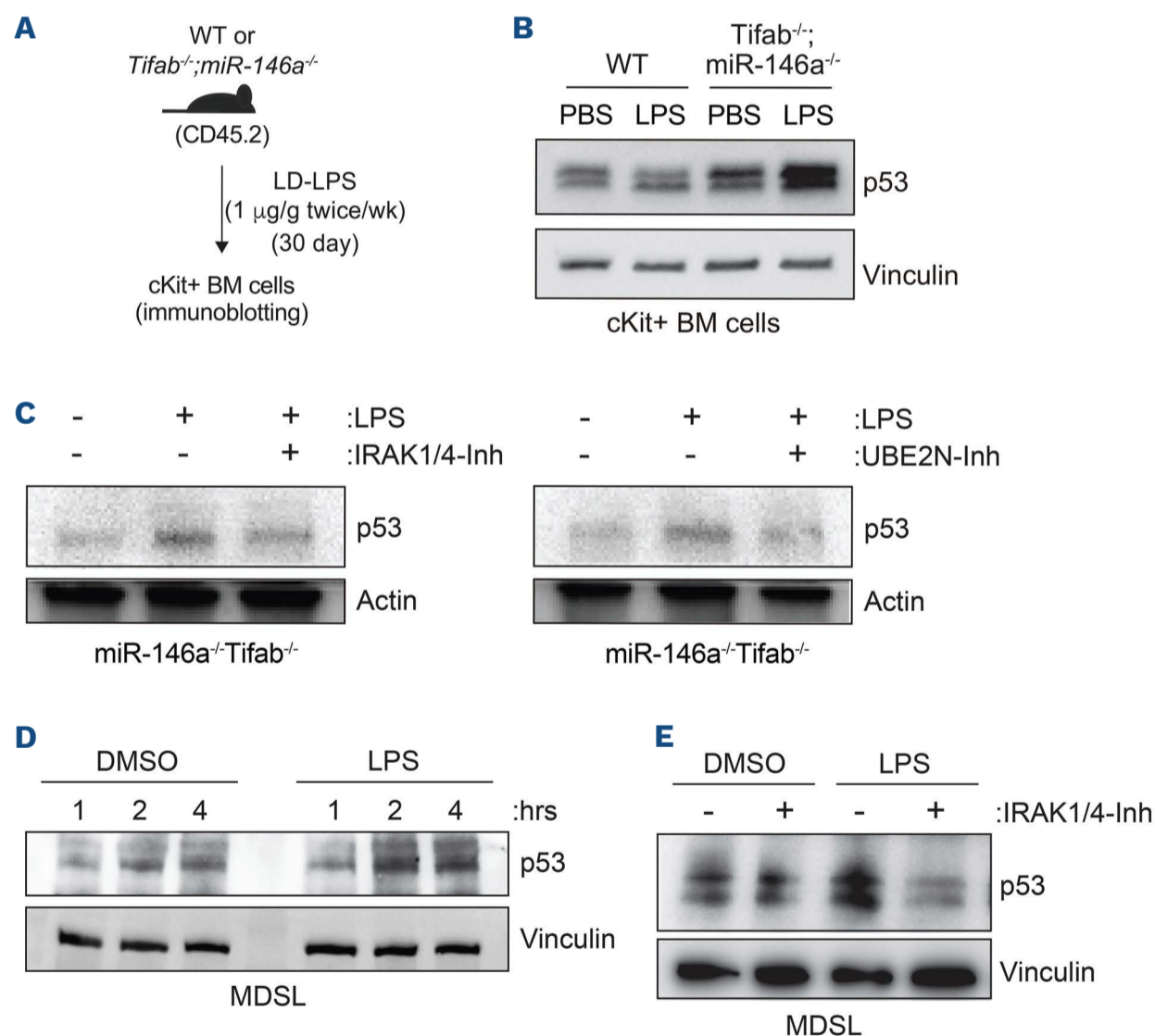


Figure 6. Low-dose lipopolysaccharide induces p53 expression in *Tifab*^{-/-};*miR-146a*^{-/-} hematopoietic stem and progenitor cells via IRAK1/4-TRAF6. (A) Outline of *in vivo* administration of lipopolysaccharide (LPS) following by immunoblot analysis. (B) Immunoblot analysis of wild-type (WT) and *Tifab*^{-/-};*miR-146a*^{-/-} c-Kit⁺ bone marrow (BM) cells from WT and *Tifab*^{-/-};*miR-146a*^{-/-} mice treated with low-dose LPS (LD-LPS) (1 μg /g) or vehicle twice a week for 30 days. (C) Immunoblotting of *Tifab*^{-/-};*miR-146a*^{-/-} BM cells treated with LPS (1 mg/mL) and the IRAK1/4 (1 mM) or UBE2N (5 mM) inhibitor for 60 minutes. (D) Immunoblot analysis of a patient-derived del(5q) myelodysplastic syndromes (MDS) cell lines (MDSL) was treated with LPS (100 ng/mL) for the indicated time points. (E) Immunoblot analysis of MDSL cells treated with LPS (100 ng/mL) and the IRAK1/4 inhibitor (1 mM) for 2 hours.

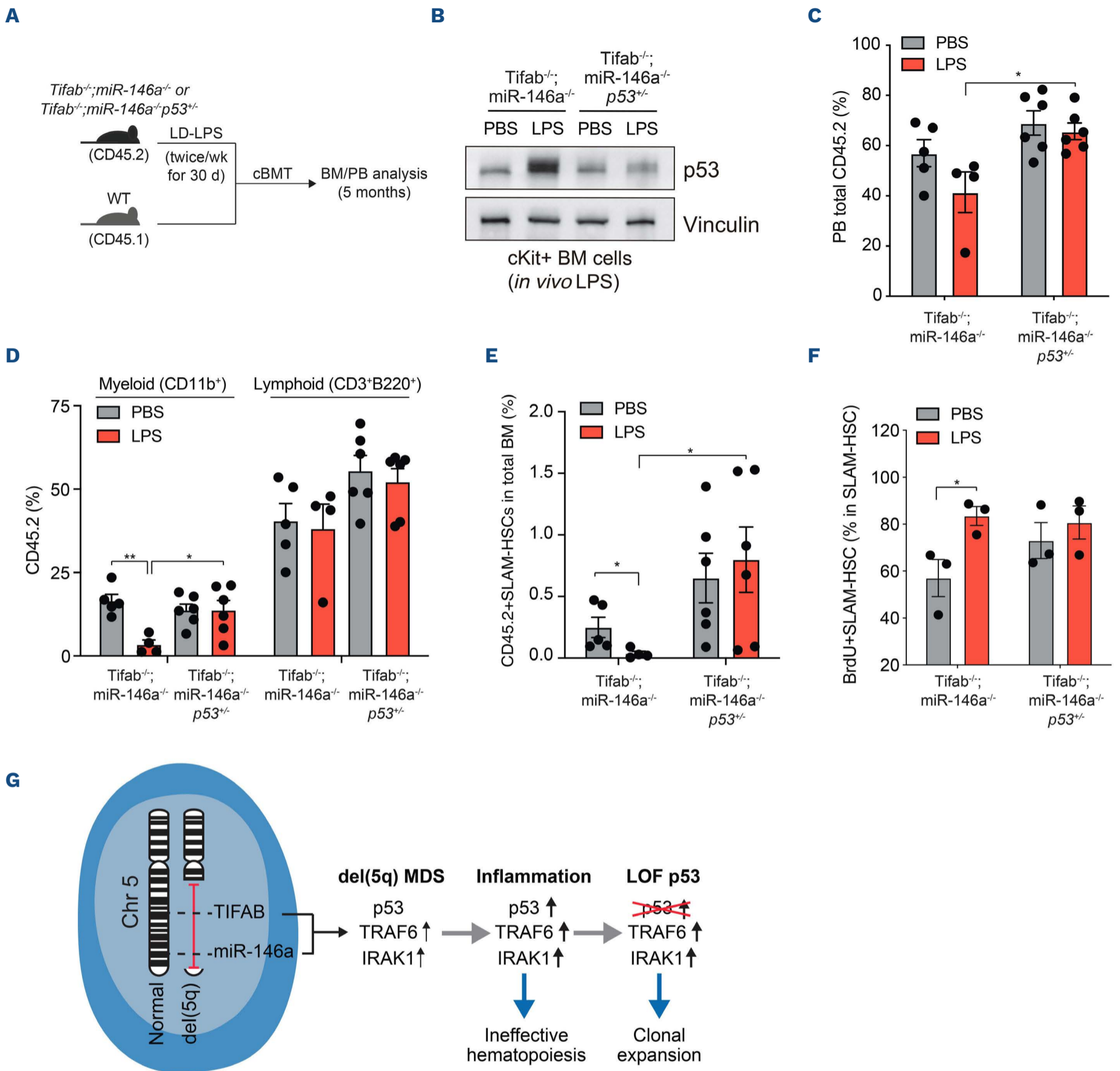


Figure 7. Deletion of p53 restores exhaustion of *Tifab*^{-/-};*miR-146a*^{-/-} hematopoietic stem cells following low-dose lipopolysaccharide. (A) Outline of competitive bone marrow (BM) transplantations using *Tifab*^{-/-};*miR-146a*^{-/-} or *Tifab*^{-/-};*miR-146a*^{-/-};*p53*^{+/-} mice in the presence of low-dose chronic inflammation. (B) Immunoblot analysis of *Tifab*^{-/-};*miR-146a*^{-/-} or *Tifab*^{-/-};*miR-146a*^{-/-};*p53*^{+/-} c-Kit⁺ BM cells from wild-type (WT) and *Tifab*^{-/-};*miR-146a*^{-/-} mice treated with low-dose lipopolysaccharide (LD-LPS) (1 μg/g) or vehicle twice a week for 30 days. (C, D) Proportion of donor-derived peripheral blood (PB) cells from the recipient mice transplanted with *Tifab*^{-/-};*miR-146a*^{-/-} or *Tifab*^{-/-};*miR-146a*^{-/-};*p53*^{+/-} mice treated with either phosphate-buffered saline (PBS) or LPS. Error bars represent the standard error of the mean (SEM). (E) Proportion of donor-derived SLAM hematopoietic stem cells (HSC) in total cells from the recipient mice transplanted with *Tifab*^{-/-};*miR-146a*^{-/-} or *Tifab*^{-/-};*miR-146a*^{-/-};*p53*^{+/-} mice treated with either PBS or LPS. Error bars represent the SEM. (F) Proportion of bromouridine (BrdU)-positive cells within HSC from *Tifab*^{-/-};*miR-146a*^{-/-} or *Tifab*^{-/-};*miR-146a*^{-/-};*p53*^{+/-} mice treated with LPS (N=3 per group). Error bars represent the SEM. (G) Summary of findings. Del(5q) myelodysplastic syndromes (MDS) hematopoietic stem and progenitor cells (HSPC) (blue) exhibit impaired hematopoiesis and increased innate immune signaling because of derepression of TRAF6 and IRAK1 following deletion of miR-146a and TIFAB. Loss of TIFAB also results in increased p53 activation due to diminished USP15 activation. During inflammation, del(5q) MDS HSPC activated IRAK-TRAF6 signaling and induce p53, which results in clonal depletion. Loss-of-function mutations (LOF) or deletion of p53 permits clonal expansion of del(5q) MDS HSPC during inflammation. Significance for panels (C, D, E, and F) was determined with a Student's *t* test (**P*<0.05).

suppression of innate immune signaling by targeting IRAK1/4 or TRAF6-UBE2N improved cytopenias, we observed that low-grade inflammation via TLR/IL1R superfamily in the del(5q)-like MDS model did not contribute to more severe disease but instead impaired the function of del(5q)-like HSPC. Unexpectedly, the functional defect of del(5q) HSPC exposed to the TLR4 ligand LPS, including their attrition following excessive proliferation, was restored by p53 deletion. Since TP53 mutations are enriched in del(5q) AML following an MDS diagnosis, increased p53 activation in del(5q) MDS HSPC due to inflammation may create a selective pressure for genetic inactivation of p53 or expansion of a pre-existing TP53-mutant clone (Figure 7G).

The prevalence of TP53 mutations in all MDS subtypes is low, averaging 5–10%, but is highly associated with isolated del(5q) or complex karyotypes with -5/5q-.^{44,49} TP53 mutations are a predictor of poor prognosis in both *de novo* and secondary MDS and are associated with higher-risk disease, p53 protein overexpression, increased blast count and AML progression.^{44,50} An isolated del(5q) in MDS has a better prognosis as compared to the other MDS cytogenetic subtypes. However, TP53 mutations occur in lower-risk del(5q) MDS at a frequency of approximately 20% and are associated with a dismal prognosis.⁴⁴ Disease progression of lower-risk del(5q) MDS is related to the evolution of pre-existing or emerging subclones carrying a TP53 mutation.⁵¹ TP53 mutations at diagnosis are predictive of disease progression in lower risk del(5q) MDS and disease progression mostly occurred in patients with TP53 mutations emerging before or at the time of progression. However, it was observed in certain cases that the absence of a TP53 mutation at diagnosis suggesting that the TP53 mutations are secondary events in del(5q) MDS patients. In line with our reported findings, increased p53 protein expression in lower risk del(5q) MDS predicts shorter overall survival and disease progression.⁵² The del(5q) MDS patients with the highest level of p53 protein expression reflect mutant TP53, suggesting there are selective pressures that lead to TP53 inactivating mutations in the del(5q) MDS clones.

It is also well established that p53 mutations are acquired in hematopoietic cells in patients receiving genotoxic therapy, leading to therapy-related MDS or AML. In this scenario, the genotoxic stress is a selective pressure for loss of p53-mediated apoptosis in the hematopoietic cells. However, the reasons for the high frequency of p53 mutations in del(5q) and which of the p53 functions are essential in del(5q) MDS is insufficiently understood. Moreover, it also remains unresolved why these p53 functions are selected against during clonal evolution and disease progression. Paradoxically, elevated p53 levels in del(5q)-like MDS HSPC following inflammation correlate with increased HSC proliferation and a reduced competitive ad-

vantage, while monoallelic loss of p53 in these cells results in reduced HSC proliferation and an increased competitive advantage. A similar effect was observed in a mouse model of hyperactive p53.⁴⁶ Hyperactive p53 results in reduced numbers of proliferating HSC in aged mice. These paradoxical observations related to p53 activity and HSPC function may be explained by the unique dependency of p53 in the context of del(5q)-like MDS HSPC within an aged and/or inflammatory milieu.

Low-grade inflammation following LPS administration results in fewer number and more proliferative *Tifab*^{-/-}; *miR-146a*^{-/-} HSC. In order to overcome the negative effects of inflammation, we posit that *Tifab*^{-/-}; *miR-146a*^{-/-} HSC have a proclivity to gain a competitive advantage upon loss of p53. TIFAB has previously been implicated in p53 regulation by directly regulating USP15 activity.³¹ Expression of TIFAB in HSPC permits USP15 signaling to substrates, including MDM2, and mitigates p53 expression in leukemic myeloid cells. As such, TIFAB-deficient HSPC exhibit compromised USP15 signaling and are sensitized to a variety of hematopoietic stressors by derepression of p53. Thus, our finding that loss of miR-146a and TIFAB in HSC results in increased p53 expression during inflammation is likely due to a cooperative effect through both del(5q) genes. Interestingly, deletion of p53 in *Tifab*^{-/-}; *miR-146a*^{-/-} HSC did not result in overt leukemia, suggesting that the primary consequence of monoallelic p53 loss is to provide del(5q) MDS HSC a competitive advantage during low-grade inflammation. Additional del(5q) genes could cooperate with loss of p53 to manifest overt leukemia. As the current study focused on two del(5q)-related genes, miR-146a and TIFAB, it likely that additional genes within the deleted segment on chr 5q also contribute to the functional consequences of inflammation in del(5q) MDS.

Increased innate immune signaling in del(5q) MDS HSPC is attributed to several haploinsufficient genes. The individual contribution of each of these haploinsufficient genes to MDS phenotypes has been extensively evaluated in mouse models.¹⁻³ More recently, various models were generated to examine the cooperation of multiple del(5q) genes. Mice lacking miR-143 and miR-145 have impaired HSPC activity with depletion of functional HSC, but activation of progenitor cells.⁵³ Lam *et al.* identified components of the transforming growth factor β (TGF β) pathway as key targets of miR-143 and miR-145. As expected, the combined deletion of miR-146a with RPS14 and CSNK1A1 recapitulated many cardinal features of del(5q) MDS, including more severe anemia with faster kinetics than Rps14 haploinsufficiency alone and pathognomonic megakaryocyte morphology.¹⁸ Combined hematopoietic-specific deletion of *Tifab* and miR-146a resulted in more rapid and severe cytopenia, and progression to a fatal BM failure-like disease as compared with *Tifab*- or miR-146a-deficiency alone.²⁵ Dual deficiency of mDia1 and

miR-146a caused an age-related anemia and ineffective erythropoiesis mimicking human MDS.⁵⁴ It was also demonstrated that the aging BM microenvironment was important for the development of ineffective erythropoiesis in these mice. Of note, loss of miR-146a alone is sufficient to induce HSC defects and hematopoietic disease.^{55,56} Deletion of miR-146a in HSC promotes premature HSC aging and inflammation, preceding development of aging-associated myeloid malignancy. These effects are mediated in part by excessive signaling through its targets TRAF6 and IRAK1. Collectively, these findings confirm that aberrant innate immune signaling in del(5q) MDS HSC and altered responses to the inflammatory microenvironment play a critical role in the pathogenesis and complex phenotype of myeloid malignancies.

Several attempts are being pursued to restore normal innate immune signaling in MDS HSC. One approach has been to inhibit IRAK4.⁵⁷ There are ongoing clinical studies evaluating IRAK4 inhibitors for low-risk MDS patients, which will provide insight into the clinical benefit of suppressing cell-intrinsic innate immune signaling pathways downstream of IRAK-TRAF6. In our study, we utilized IRAK1/4 and UBE2N inhibitors, which individually improved the anemia in the del(5q)-like MDS model. Moreover, it is also possible that suppressing chronic inflammation in low-risk del(5q) MDS patients may diminish the selective pressures leading to acquired p53 mutations. Such an approach has been demonstrated experimentally wherein the selective pressure against p53 in models of lymphoma can be mitigated by targeting the apoptotic pathway.⁵⁸ Therefore, future studies should determine whether mitigating inflammation in del(5q) MDS may reduce the likelihood of secondary p53 mutations and progression towards more aggressive disease.

Disclosures

DTS serves on the scientific advisory board at Kurome Therapeutics and is a consultant for and/or received funding

from Kurome Therapeutics, Captor Therapeutics, Treeline Biosciences, and Tolero Therapeutics. DTS has equity in Kurome Therapeutics. The other authors have no conflicts of interest to disclose.

Contributions

TM performed experiments, analyzed and interpreted data, and wrote the manuscript. CSW performed experiments, analyzed and interpreted data, and contributed to writing the manuscript. PA, EV, KC, MN, CI, KH, AS and MV performed experiments and analyzed and interpreted data. TM and DTS conceived and directed the study, analyzed and interpreted data, and wrote and/or edited the manuscript. All authors approved the final version of the manuscript.

Funding

This work was supported in parts by the National Institute of Health (U54DK126108, R35HL166430, R01CA271455, R01CA275007), Cincinnati Children's Hospital Research Foundation, Cancer Free Kids, and Blood Cancer Discoveries Grant program through The Leukemia & Lymphoma Society, The Mark Foundation for Cancer Research and The Paul G. Allen Frontiers Group to DTS. TM was supported by The Uehara Memorial Foundation, The Waksman Foundation of Japan, The Mochida Memorial Foundation for Medical and Pharmaceutical Research, Japan Society for the Promotion of Science, and Ohio State University Comprehensive Cancer Center. TM was a Leukemia and Lymphoma Society Special Fellow. EV was supported by an NIH Institutional Research Training Grant (T32CA236764).

Data-sharing statement

Cell lines and mouse models used in these studies are publicly available through commercial sources or may be made available from the authors upon written request and material transfer agreement approval. The authors are also glad to share guidance regarding protocols and assays used in these studies upon written request.

References

1. Trowbridge JJ, Starczynowski DT. Innate immune pathways and inflammation in hematopoietic aging, clonal hematopoiesis, and MDS. *J Exp Med*. 2021;218(7):e20201544.
2. Barreyro L, Chlon TM, Starczynowski DT. Chronic immune response dysregulation in MDS pathogenesis. *Blood*. 2018;132(15):1553-1560.
3. Stubbins RJ, Platzbecker U, Karsan A. Inflammation and myeloid malignancy: quenching the flame. *Blood*. 2022;140(10):1067-1074.
4. Cai Z, Kotzin JJ, Ramdas B, et al. Inhibition of inflammatory signaling in Tet2 mutant preleukemic cells mitigates stress-induced abnormalities and clonal hematopoiesis. *Cell Stem Cell*. 2018;23(6):833-849.
5. Higa KC, Goodspeed A, Chavez JS, et al. Chronic interleukin-1 exposure triggers selection for Cebpa-knockout multipotent hematopoietic progenitors. *J Exp Med*. 2021;218(6):e20200560.
6. Reynaud D, Pietras E, Barry-Holson K, et al. IL-6 controls leukemic multipotent progenitor cell fate and contributes to chronic myelogenous leukemia development. *Cancer Cell*. 2011;20(5):661-673.
7. Hemmati S, Haque T, Gritsman K. Inflammatory signaling pathways in preleukemic and leukemic stem cells. *Front Oncol*. 2017;7:265.
8. Avagyan S, Henninger JE, Mannherz WP, et al. Resistance to inflammation underlies enhanced fitness in clonal hematopoiesis. *Science*. 2021;374(6568):768-772.
9. Muto T, Walker CS, Choi K, et al. Adaptive response to inflammation contributes to sustained myelopoiesis and confers a competitive advantage in myelodysplastic syndrome

- HSCs. *Nat Immunol.* 2020;21(5):535-545.
10. Liao M, Chen R, Yang Y, et al. Aging-elevated inflammation promotes DNMT3A R878H-driven clonal hematopoiesis. *Acta Pharm Sin B.* 2022;12(2):678-691.
 11. Zhang CR, Ostrand EL, Kukhar O, et al. Txnip enhances fitness of Dnmt3a-mutant hematopoietic stem cells via p21. *Blood Cancer Discov.* 2022;3(3):220-239.
 12. Hormaechea-Agulla D, Matatall KA, Le DT, et al. Chronic infection drives Dnmt3a-loss-of-function clonal hematopoiesis via IFN γ signaling. *Cell Stem Cell.* 2021;28(8):1428-1442.
 13. Qian Z, Joslin JM, Tennant TR, et al. Cytogenetic and genetic pathways in therapy-related acute myeloid leukemia. *Chem Biol Interact.* 2010;184(1-2):50-57.
 14. Haase D. Cytogenetic features in myelodysplastic syndromes. *Ann Hematol.* 2008;87(7):515-526.
 15. Haase D, Germing U, Schanz J, et al. New insights into the prognostic impact of the karyotype in MDS and correlation with subtypes: evidence from a core dataset of 2124 patients. *Blood.* 2007;110(13):4385-4395.
 16. Ebert BL, Pretz J, Bosco J, et al. Identification of RPS14 as a 5q-syndrome gene by RNA interference screen. *Nature.* 2008;451(7176):335-339.
 17. Schneider RK, Schenone M, Ferreira MV, et al. Rps14 haploinsufficiency causes a block in erythroid differentiation mediated by S100A8 and S100A9. *Nat Med.* 2016;22(3):288-297.
 18. Ribezzo F, Snoeren IAM, Ziegler S, et al. Rps14, Csnk1a1 and miRNA145/miRNA146a deficiency cooperate in the clinical phenotype and activation of the innate immune system in the 5q- syndrome. *Leukemia.* 2019;33(3):1759-1772.
 19. Stalman USA, Ticconi F, Snoeren IAM, et al. Genetic barcoding systematically compares genes in del(5q) MDS and reveals a central role for CSNK1A1 in clonal expansion. *Blood Adv.* 2022;6(6):1780-1796.
 20. Keerthivasan G, Mei Y, Zhao B, Zhang L, Harris CE, Gao J et al. Aberrant overexpression of CD14 on granulocytes sensitizes the innate immune response in mDia1 heterozygous del(5q) MDS. *Blood.* 2014;124(5):780-790.
 21. Kumar MS, Narla A, Nonami A, et al. Coordinate loss of a microRNA and protein-coding gene cooperate in the pathogenesis of 5q- syndrome. *Blood.* 2011;118(17):4666-4673.
 22. Starczynowski DT, Kuchenbauer F, Argiropoulos B, et al. Identification of miR-145 and miR-146a as mediators of the 5q-syndrome phenotype. *Nat Med.* 2010;16(1):49-58.
 23. Fang J, Barker B, Bolanos L, et al. Myeloid malignancies with chromosome 5q deletions acquire a dependency on an intrachromosomal NF- κ B gene network. *Cell Rep.* 2014;8(5):1328-1338.
 24. Rhyasen GW, Bolanos L, Fang J, et al. Targeting IRAK1 as a therapeutic approach for myelodysplastic syndrome. *Cancer Cell.* 2013;24(1):90-104.
 25. Varney ME, Choi K, Bolanos L, et al. Epistasis between TIFAB and miR-146a: neighboring genes in del(5q) myelodysplastic syndrome. *Leukemia.* 2017;31(2):491-495.
 26. Varney ME, Niederkorn M, Konno H, et al. Loss of Tifab, a del(5q) MDS gene, alters hematopoiesis through derepression of Toll-like receptor-TRAF6 signaling. *J Exp Med.* 2015;212(11):1967-1985.
 27. Fang J, Bolanos LC, Choi K, et al. Ubiquitination of hnRNPA1 by TRAF6 links chronic innate immune signaling with myelodysplasia. *Nat Immunol.* 2017;18(2):236-245.
 28. Starczynowski DT, Morin R, McPherson A, et al. Genome-wide identification of human microRNAs located in leukemia-associated genomic alterations. *Blood.* 2011;117(2):595-607.
 29. Boldin MP, Taganov KD, Rao DS, et al. miR-146a is a significant brake on autoimmunity, myeloproliferation, and cancer in mice. *J Exp Med.* 2011;208(6):1189-1201.
 30. Zhao JL, Rao DS, Boldin MP, Taganov KD, O'Connell RM, Baltimore D. NF- κ B dysregulation in microRNA-146a-deficient mice drives the development of myeloid malignancies. *Proc Natl Acad Sci U S A.* 2011;108(22):9184-9189.
 31. Niederkorn M, Hueneman K, Choi K, et al. TIFAB regulates USP15-mediated p53 signaling during stressed and malignant hematopoiesis. *Cell Rep.* 2020;30(8):2776-2790.
 32. Melgar K, Walker MM, Jones LM, Bolanos LC, Hueneman K, Wunderlich M et al. Overcoming adaptive therapy resistance in AML by targeting immune response pathways. *Sci Transl Med.* 2019;11(508):eaaw8828.
 33. Jones LM, Melgar K, Bolanos L, et al. Targeting AML-associated FLT3 mutations with a type I kinase inhibitor. *J Clin Invest.* 2020;130(508):2017-2023.
 34. Barreyro L, Sampson AM, Ishikawa C, et al. Blocking UBE2N abrogates oncogenic immune signaling in acute myeloid leukemia. *Sci Transl Med.* 2022;14(635):eabb7695.
 35. Fang J, Liu X, Bolanos L, et al. A calcium- and calpain-dependent pathway determines the response to lenalidomide in myelodysplastic syndromes. *Nat Med.* 2016;22(7):727-734.
 36. Rhyasen GW, Wunderlich M, Tohyama K, Garcia-Manero G, Mulloy JC, Starczynowski DT. An MDS xenograft model utilizing a patient-derived cell line. *Leukemia.* 2014;28(5):1142-1145.
 37. Fang J, Muto T, Kleppe M, et al. TRAF6 mediates basal activation of NF- κ B necessary for hematopoietic stem cell homeostasis. *Cell Rep.* 2018;22(5):1250-1262.
 38. Muto T, Guillamot M, Yeung J, et al. TRAF6 functions as a tumor suppressor in myeloid malignancies by directly targeting MYC oncogenic activity. *Cell Stem Cell.* 2022;29(2):298-314.
 39. Chlon TM, Stepanchick E, Hershberger CE, et al. Germline DDX41 mutations cause ineffective hematopoiesis and myelodysplasia. *Cell Stem Cell.* 2021;28(11):1966-1981.
 40. Schuettpelz LG, Link DC. Regulation of hematopoietic stem cell activity by inflammation. *Front Immunol.* 2013;4:204.
 41. Wang R, Yang X, Liu J, et al. Gut microbiota regulates acute myeloid leukaemia via alteration of intestinal barrier function mediated by butyrate. *Nat Commun.* 2022;13(1):2522.
 42. Takizawa H, Fritsch K, Kovtonyuk LV, et al. Pathogen-induced TLR4-TRIF innate immune signaling in hematopoietic stem cells promotes proliferation but reduces competitive fitness. *Cell Stem Cell.* 2017;21(2):225-240.
 43. Esplin BL, Shimazu T, Welner RS, et al. Chronic exposure to a TLR ligand injures hematopoietic stem cells. *J Immunol.* 2011;186(9):5367-5375.
 44. Zhang L, McGraw KL, Sallman DA, List AF. The role of p53 in myelodysplastic syndromes and acute myeloid leukemia: molecular aspects and clinical implications. *Leuk Lymphoma.* 2017;58(8):1777-1790.
 45. Bernard E, Nannya Y, Hasserjian RP, et al. Implications of TP53 allelic state for genome stability, clinical presentation and outcomes in myelodysplastic syndromes. *Nat Med.* 2020;26(10):1549-1556.
 46. Dumble M, Moore L, Chambers SM, et al. The impact of altered p53 dosage on hematopoietic stem cell dynamics during aging. *Blood.* 2007;109:1736-1742.
 47. Nielsen AB, Hansen JW, Orskov AD, et al. Inflammatory cytokine profiles do not differ between patients with idiopathic cytopenias of undetermined significance and myelodysplastic syndromes. *Hemasphere.* 2022;6(5):e0713.
 48. Riello GBC, Mendonça da Silva P, da Silva Oliveira FA, et al. Gut microbiota composition correlates with disease severity in myelodysplastic syndrome. *medRxiv.* 2022 Apr 18.

- doi: 10.1101/2022.04.18.22273768 [preprint, not peer-reviewed]
49. Hosono N, Makishima H, Mahfouz R, et al. Recurrent genetic defects on chromosome 5q in myeloid neoplasms. *Oncotarget*. 2017;8(4):6483-6495.
50. Jadersten M, Saft L, Smith A, et al. TP53 mutations in low-risk myelodysplastic syndromes with del(5q) predict disease progression. *J Clin Oncol*. 2011;29(15):1971-1979.
51. Lode L, Menard A, Flet L, et al. Emergence and evolution of TP53 mutations are key features of disease progression in myelodysplastic patients with lower-risk del(5q) treated with lenalidomide. *Haematologica*. 2018;103(4):e143-e146.
52. Saft L, Karimi M, Ghaderi M, et al. p53 protein expression independently predicts outcome in patients with lower-risk myelodysplastic syndromes with del(5q). *Haematologica*. 2014;99(6):1041-1049.
53. Lam J, van den Bosch M, Wegrzyn J, et al. miR-143/145 differentially regulate hematopoietic stem and progenitor activity through suppression of canonical TGF β signaling. *Nat Commun*. 2018;9(1):2418.
54. Mei Y, Zhao B, Basiorka AA, et al. Age-related inflammatory bone marrow microenvironment induces ineffective erythropoiesis mimicking del(5q) MDS. *Leukemia*. 2018;32(4):1023-1033.
55. Grants JM, Wegrzyn J, Hui T, et al. Altered microRNA expression links IL6 and TNF-induced inflammaging with myeloid malignancy in humans and mice. *Blood*. 2020;135(25):2235-2251.
56. Zhao JL, Rao DS, Boldin MP, Taganov KD, O'Connell RM, Baltimore D. NF-kappaB dysregulation in microRNA-146a-deficient mice drives the development of myeloid malignancies. *Proc Natl Acad Sci U S A*. 2011;108:9184-9189.
57. Bennett J, Starczynowski DT. IRAK1 and IRAK4 as emerging therapeutic targets in hematologic malignancies. *Curr Opin Hematol*. 2022;29(1):8-19.
58. Lu X, Yang C, Yin C, Van Dyke T, Simin K. Apoptosis is the essential target of selective pressure against p53, whereas loss of additional p53 functions facilitates carcinoma progression. *Mol Cancer Res*. 2011;9(4):430-439.